

# MECHANICAL ANTHROPOGENIC IMPACT ON NATURAL SLOPES OF COASTAL DUNES

A. R. Danchenkov<sup>1,2,\*</sup> , E. D. Piterniex<sup>1,2</sup> , and N. S. Belov<sup>2</sup> 

<sup>1</sup> Shirshov Institute of Oceanology, Russian Academy of Sciences, Kaliningrad, Russia

<sup>2</sup> Immanuel Kant Baltic Federal University, Kaliningrad, Russia

\* **Correspondence to:** Aleksandr Danchenkov, aldanchenkov@mail.ru

**Abstract:** The results of a series of experimental works on controlled human trampling on natural slopes of coastal dunes are summarized. Intensification of anthropogenic impact on coastal dunes, including the growth of local tourism, together with modern climatic changes, leads to degradation of coastal aeolian-marine complexes. The impact of human foot traffic on dune slopes triggers a chain of morphodynamic processes that ultimately lead to sand activation and migration. The morphodynamic effect of human trampling depends on the initial moisture content of the sand and the depth of the dried layer, which expires in streams before reaching the natural slope and leads to a localized change in moisture content due to instantaneous mixing. The morphodynamic effect of multiple successive human descents is to form a trough of disturbed sands, within which there is a slow outflow of dry sand moved by slow displacement. In both cases, the displacement process is similar to that of a “flowing wedge”, where under the action of surface pressure in a local depression there is a correlated movement of particles confined to a region defined by the length of the stress chains. The processes of subsequent relaxation cause the crumbling of microform walls of the footprint formed by the moistened sand layer and the formation of the natural slope in new, “shifted”, conditions.

**Keywords:** Coastal dune, Trampling, Dune slopes, Geometric transformation vector, Morphodynamics

**Citation:** Danchenkov A. R., Piterniex E. D., Belov N. S. (2025), Mechanical Anthropogenic Impact on Natural Slopes of Coastal Dunes, *Russian Journal of Earth Sciences*, 25, ES5027, EDN: HRFLZE, <https://doi.org/10.2205/2025es001026>

## 1. Introduction

Direct mechanical degradation of natural slopes by human walking can be considered the most noticeable type of recreational impact on open sandy slopes of coastal dunes. As a beach holiday, active tourism on the seashore, bivouac tourism, especially with children in the group, is accompanied by walking, jumping, trampling and climbs on sandy slopes, it has a diverse impact on the stability of the aeolian forms [Defeo *et al.*, 2009; Liddle and Greig-Smith, 1975; Pessoa and Lidon, 2013]. Human activity and the resulting changes in coastal landscapes have undergone rapid growth with the development of society, the emergence of mechanization means and population increase [Nordstrom, 2000]. Previously, the effects caused by human movement through the dunes were mainly considered as indirect – such as the creation of paths, damage to cover and waste disposal [Mather and Ritchie, 1977]. However, as tourism activity increases, the increased frequency of mechanical impact (moving more people on slopes) produces a greater aggregate effect. Thus, the minor factors that contributed to the negative morphodynamic effects on coastal dunes intensified in the 20th century and continue to have an increasing influence on their development [Acosta *et al.*, 2013; Hesp, 2024].

Coastal cities are heavily dependent on the recreational use of beaches, which in good times attract both local and incoming tourists, which is reflected in the increased rate of their degradation. For medium and low latitudes, the disturbed areas have only

## RESEARCH ARTICLE

Received: December 18, 2024

Accepted: May 22, 2025

Published: December 24, 2025



**Copyright:** © 2025. The Authors. This article is an open access article distributed under the terms and conditions of the Creative Commons Attribution (CC BY) license (<https://creativecommons.org/licenses/by/4.0/>).

a small interval to recover before they will be breached again in high season [Pessoa and Lidon, 2013]. This leads to the formation of corridors which, in a stormy period, due to natural narrowing and greater erosion instability (changes in moisture stratification and sand density) at a lower threshold shear velocity of particles, are subject to deflation and stimulate the formation of blowouts. The increase in storm activity and climate change in the Kaliningrad region [Stont et al., 2023a,b] will naturally influence the intensification of such phenomena and increase the volume of sand inflow by means of aeolian transport through the created corridors, threatening the infrastructure. Such threats together with a number of other factors provoke changes in the morphological structure of coastal dunes, activate erosion processes and cause changes in the structures of plant communities [Cogoni et al., 2024; Fenu et al., 2013].

Studies on the impact of human activity on slopes are widely represented in ecological and biological works on the response of flora and fauna to walking, reviewed in the study by Ravichandran and Rashid [2017]. Experimental studies were conducted for parabolic dunes taking into account the morphology of the dune slope [Hesp et al., 2010]. Mass fluxes caused by wind erosion have been assessed for disturbed walking soils taking into account physical and biological factors. Even moderate surface disturbance leads to significant soil loss, which can have long-term negative consequences for the ecosystem [Belnap et al., 2007].

In the context of increasing tourist demand, it is necessary to regularly update information on the protection status of coastal dunes by inputting and outputting from use some of their areas [Pinna et al., 2019]. To determine the effect of one of the most common types of anthropogenic impact on coastal dunes, it is necessary to have quantitative knowledge of the processes involved.

The aim of this work is to evaluate the morphodynamic potential of mechanical anthropogenic impact in exposed sandy surfaces of coastal dune slopes. For this purpose, discrete experimental descents and sampling accompanied by terrestrial laser scanning (TLS) were carried out, as well as studies of links of the geometric transformation vector with the geomorphological and lithological properties of sand, and the effects of relaxation on the movement of sand masses after impact.

## 2. Materials and methods

### 2.1. Morphodynamic experiments

The experimental work was carried out on 9 natural sandy slopes of the coastal dunes of Vistula Spit and Malinovka village (Zelenogradsk district) in 2020 to 2024 in different seasons of the year and preceding them intense storm events (Figure 1). This allowed to cover a wide range of sand moisture (0.1% to 5%) and ensure an unbroken initial state of the sand profile.

A cross-section from the crest to the base of the foredune or dune ridge was laid for the descents. The location of the object on the slope of the dune was determined based on the practical feasibility of geomorphological conditions for optimal use of this surface by vacationers as a descent. The slope height was 7 m to 10 m, used both windward and leeward slopes of the dunes.

The descent was carried out by simulating the person's walk and the length of his step (0.5 m to 0.6 m). Usually to save energy when moving on a sandy slope, the person seeks to perform minimal muscular actions by producing a controlled fall, which is expressed in stamp-like impacts on the surface of the sand. In the experimental studies, both isolated single impacts designed to assess basic changes and a series of consecutive impacts simulating a long-lasting dynamic load were implemented. The maximum number of cycles in a single series was 42. The focus of subsequent analysis was on an intermediate range of no more than ten impacts. It was assumed that the effects most relevant to typical interaction scenarios with the studied environment are expressed in this interval. The criterion for determining a significant range of impact cycles (up to 10) was an empirical

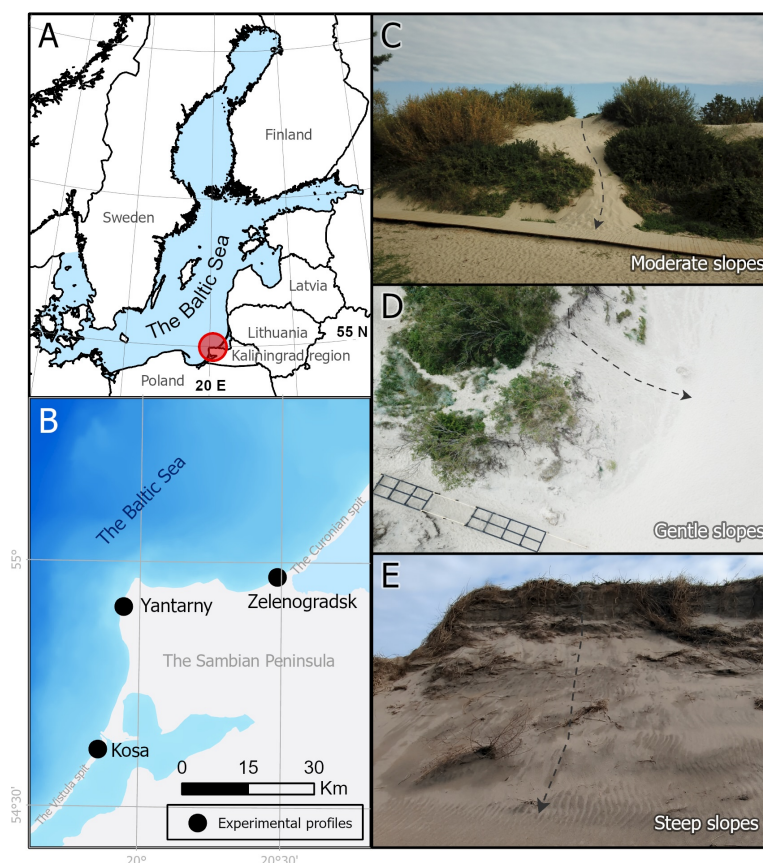


**Figure 1.** A, B – location of the study area and sites; C, D, E – typical examples of profiles involved in the study.

assessment of the average activity of the vacationers group moving along the examined surface in the direction of the beach area.

The sampling of sand was carried out before the descent ( $M_0$ ) on the axis of the intended descent route, as well as directly after the descent ( $M_i$ ). Index  $i$  here and further expresses the number of descents on the track. The top layer of sand 0 cm to 7 cm, weighing 0.5 kg, was collected in a glass jar.

In order to evaluate the effect of short-term impact of drying freshly exposed sands, successive selections were made according to the scheme:  $M_0$ ;  $M_{i=1}$ ;  $M_{i=1} + 30$  minutes.

## 2.2. Sampling and analysis

The moisture content (percentage mass content of moisture in the sample) was determined using a  $\pm 0.01$  g laboratory balance and a desiccator at  $120^\circ\text{C}$  with a 200 g sample. In order to determine the values of low-moisture samples, an increased sample volume of up to 0.5 kg was used. For each sample, the moisture anomaly  $M_a$  relative to the initial moisture  $M_0$  in the corresponding series was determined by the formula (Equation 1):

$$M_a = M_i - M_0, \quad (1)$$

where  $M_0$  is the initial moisture (before the descents),  $M_i$  is the sample moisture after the descents.

For the samples, a granulometric analysis was carried out by dry sieve sieving on sieves 1; 0.5; 0.4; 0.315; 0.25; 0.1 and 0.063 mm using a Fritch vibrating screen and laboratory analytical balances. The integration of results into GRADISTAT [Blott and Pye, 2001] allowed to perform calculations of median diameter ( $D_{50}$ , mm) and sorting (geometric

value,  $\mu\text{m}$ ) according to Folk & Ward method [Folk and Ward, 1957] for interpretation of changes in lithological composition under the impact of human trampling.

### 2.3. Terrain modeling

Terrain modeling for slope morphodynamics was carried out using TLS (Topcon GLS-1500 scanner). Scanning was performed from single station, which allowed measurements in the local coordinate system. Measurements were made before the descents (or their series) and after, according to a regular scheme similar to the sampling scheme. Authors have previously used TLS for a number of coastal studies [Danchenkov and Belov, 2023; Danchenkov et al., 2023, 2019; Danchenkov and Belov, 2019].

Post-processing of the results was carried out in specialized software TOPCON ScanMaster. Subsequent processing and preparation of digital models was carried out in the GIS Esri ArcGIS Pro. The construction of a digital relief model was carried out using the Natural neighbor method [Sibson, 1981] with a 0.05 m cell.

Calculation of changes is the first task when assessing the development of landforms over time [Williams, 2012]. Analysis of digital elevation models (DEM) is a powerful and relevant tool for studying morphodynamic processes [Burvingt and Castelle, 2023; Burvingt et al., 2017; Charbonneau et al., 2022; Danchenkov et al., 2023, 2019; Eelsalu et al., 2022; Moskalewicz et al., 2024]. Obtaining a digital elevation model of differences (DOD) is possible by subtracting the DEM obtained at an earlier point in time from the DEM obtained at a later point in time [Bannister et al., 1998], which in our particular case looks like this (Equation 2):

$$\Delta h = z_i - z_0, \quad (2)$$

where  $\Delta h$  – model showing changes in elevations after impact – DOD;  $z_0$  – DEM obtained before a descent;  $z_i$  – DEM obtained after descents in the amount of  $i$ .

The direction and intensity of the morphodynamic process were assessed through differential analysis of the difference in DEMs [Danchenkov et al., 2019]. For each cell, the rates of morphological change along the axes were determined according to the Equation 3. The discretization value (cell size) was  $c = 0.05 \text{ m}$ .

$$\begin{aligned} G_x &= \frac{d\Delta h}{dx} = \Delta h_x - \Delta h_{x-1}; \\ G_y &= \frac{d\Delta h}{dy} = \Delta h_y - \Delta h_{y-1}. \end{aligned} \quad (3)$$

The intensity of morphological changes expressed in geometric transformation vector  $\mathbf{q}(\text{m}^3/\text{c}/\text{i})$  as a consequence of the integral influence of active factors were determined according to the Equation 4:

$$q = \sqrt{G_x^2 + G_y^2}. \quad (4)$$

The physical meaning of such magnitude consists in the amount of volume (sand) that has moved between neighboring cells due to human trampling. In the conditions of such a closed morphodynamic system (all the way down the slope), the mean value of the change  $\Delta h$  corresponds to the measurement error, which causes such an analytical approach. The discretization value of  $c = 0.05 \text{ m}$  was taken, based on the typical scale of the process during field observations.

### 2.4. Calculations and statistical studies

Statistical studies were carried out to find the connection between the amount of applied impact  $i$  (number of descents in the series) and changes in moisture of the natural sandy slope  $M_a$ , as well as morphodynamic changes (geometric transformation vector), which occurred against the background of factors combination – granulometric composition and surface slope angle. Analysis of factors cumulative impact was performed by constructing models in the form of multiple linear and logarithmic regression using the smallest squares method using Microsoft Excel.

### 3. Results

To estimate the influence of descent series number on the change in the moisture content of the active layer, the materials obtained were presented in Table 1. The initial moisture of  $M_0$  varies in a fairly wide range from 0.1 to 5%. The most tested were the  $M_a$  moisture anomalies caused by a single descent as the most likely in practice, since the coincidence of traces occurs after a certain number of impacts in the series.

**Table 1.** Moisture dynamics in series of descents

Series	$M_a$ (%)	$M_0$ (%)	$I$ (pcs)	Series	$M_a$ (%)	$M_0$ (%)	$I$ (pcs)
M1	0.2	0.3	1	M21	1.6	2.2	9
M2	0.4	0.5	1	M22	1.9	3.5	9
M3	1.3	1.0	1	M23	0.3	0.5	10
M4	1.6	1.0	1	M24	0.4	1.1	10
M5	1.8	1.0	1	M25	1.3	1.2	10
M6	1.3	1.2	1	M26	1.3	1.2	10
M7	1.5	1.3	1	M27	0.4	10.7	10
M8	0.8	1.6	1	M28	1.4	0.3	14
M9	0.4	1.8	1	M29	1.4	1.2	14
M10	0.2	2.0	1	M30	1.8	1.3	14
M11	0.8	0.3	2	M31	1.4	1.2	15
M12	0.7	0.5	2	M32	0.5	2.1	15
M13	0.6	0.3	3	M33	0.4	0.4	20
M14	0.4	0.5	3	M34	1.4	1.1	20
M15	1.1	0.5	4	M35	1.5	1.1	20
M16	0.9	0.3	5	M36	1.5	1.2	20
M17	0.7	0.5	5	M37	1.5	10.7	30
M18	0.9	1.2	5	M38	0.8	2.3	36
M19	0.9	1.2	5	M39	0.4	2.8	36
M20	1.2	2.1	9	M40	2.1	2.2	42

Human trampling on open sandy slopes have a significant influence on the occurrence of the moisture anomaly  $M_a$ . The mixing process of the sand mass leads to an active redistribution of moisture, reaching an anomaly of 2.1% with 42 descents (M40 series). The most significant changes in moisture are observed at the first descents (M1–M10 series), when the moisture anomalies reach 1.8%. As the number of descents increases, there is a slowdown in the growth of the moisture anomaly associated with the involvement of the dried sand, the loss of moisture to evaporation and the retardation of the conditional growth curve reaching a value close to the maximum moisture. The mixing process is also reflected in the dynamics of granulometric composition according to the Table 2.

During trampling, there is also a change in the size of the sand on the slope. There is an increase in the median diameter after impact, increasing by 10  $\mu\text{m}$  to 30  $\mu\text{m}$ , but significant increments are observed only in two cases (L1–L3 series), which may be caused by an imbalance due to earlier secondary aeolian differentiation of exposed sands. In the process of mechanical action, there is a reduction in the degree of the sand material sorting, which also indicates the homogenization process of the initially stratified structure of the aeolian sediments. For example, a visual analysis of the vertical slice of the active layer of aeolian sand often reveals the alternation of thin layers of different shades or granulometric composition, which is direct evidence of their original layered structure.



Table 3 presents the experimental results of discrete geometric transformation vector definitions formed during impact of different intensities under conditions of different surface slope.

In Table 3, the experimental results are sorted by the number of descents  $i$  and then by the angle of the sandy slope. The smallest geometric transformation vector ( $Q = 0.5 \text{ m}^3/\text{m}$ ) (geometric transformation vector  $q(\text{m}^3/\text{c})$ , brought to a discretization value of  $0.05 \text{ m}$ ) was

**Table 2.** Main parameters of sandy slopes granulometric composition dynamics in series of descents

Series	Trampling, $i = 5$	$D_{10}$ (mm)	$D_{50}$ (mm)	$D_{90}$ (mm)	Sorting (mm)
L1	before	142.9	292.5	404.8	1.513
	after	150.1	306.6	425.9	1.485
L2	before	130.9	278.5	386.8	1.514
	after	142.6	293.7	394.8	1.474
L3	before	125.0	260.6	313.7	1.454
	after	144.4	294.8	390.2	1.433
L4	before	136.5	283.9	390.0	1.493
	after	148.7	298.5	398.3	1.454
L5	before	144.8	289.4	385.4	1.436
	after	158.6	294.1	388.9	1.386
L6	before	125.4	268.3	375.5	1.527
	after	126.6	269.2	376.6	1.507
L7	before	136.7	283.8	387.6	1.485
	after	141.6	290.4	390.6	1.470

**Table 3.** Morphological dynamics of the natural sandy dune slope

Series	$q$ ( $\text{m}^3/\text{cell}$ )	$Q$ ( $\text{m}^3/\text{m}$ )	$I$ (pcs)	Slope (degrees)	Series	$q$ ( $\text{m}^3/\text{cell}$ )	$Q$ ( $\text{m}^3/\text{m}$ )	$I$ (pcs)	Slope (degrees)
D1	0.04	0.78	1	17.4	D20	0.07	1.42	7	22.1
D2	0.04	0.78	1	22.1	D21	0.05	1.08	7	27.8
D3	0.04	0.66	1	27.8	D22	0.12	2.34	9	29.9
D4	0.09	1.84	1	30.1	D23	0.10	1.98	9	32.4
D5	0.07	1.48	1	32.6	D24	0.17	3.50	9	46.4
D6	0.12	2.26	1	47.0	D25	0.07	1.50	11	20.3
D7	0.05	0.98	2	17.4	D26	0.07	1.38	12	17.4
D8	0.05	0.92	2	22.1	D27	0.09	1.76	12	22.1
D9	0.04	0.78	2	27.8	D28	0.06	1.20	12	27.8
D10	0.06	1.14	3	20.4	D29	0.08	1.56	14	17.4
D11	0.07	1.36	5	20.4	D30	0.09	1.78	14	22.1
D12	0.03	0.50	6	7.8	D31	0.06	1.28	14	27.8
D13	0.07	1.42	6	20.4	D32	0.08	1.56	18	20.3
D14	0.07	1.48	6	23.4	D33	0.08	1.66	20	20.4
D15	0.06	1.16	6	27.9	D34	0.05	0.94	36	7.8
D16	0.12	2.28	6	30.0	D35	0.09	1.88	36	23.4
D17	0.09	1.84	6	32.5	D36	0.08	1.66	36	27.6
D18	0.15	3.00	6	46.6	D37	0.05	0.98	42	7.8
D19	0.06	1.22	7	17.4					

recorded on the least steep slopes ( $7.8^\circ$ ) with minimal applied impact (6 descents). The greatest geometric transformation vector ( $Q = 3.5 \text{ m}^3/\text{m}$ ) of material to be moved was observed on steep slopes ( $46.4^\circ$ ) as a result of 9 consecutive descents. The increase in geometric transformation vector is noticeable against the background of increasing slope angles: with equal impact, more geometric transformation vector will be formed on steep slopes. The trend of increasing geometric transformation vector due to the increase in the amount of applied impact is less obvious. These parameters may be related to the formed moisture anomaly, which determines the local physical and mechanical properties of sand.

Analysis of the dynamics of moisture desorption in sand material after experimental impact was based on a limited sample of data obtained from only five exposure cycles. The relaxation changes of moisture in the studied samples showed a limited range of values. However, the data obtained allowed an indicative estimation of the rate of short-term moisture desorption after mechanical impact simulating pedestrian load (Table 4).

**Table 4.** Dynamics of sand moisture after impact

Series	$M_0$ (%)	$M_i = 1$ (%)	$M_i = 1 + 30$ minutes (%)
R1	1.2	2.5	2.1
R2	1.3	2.8	2.1
R3	1.6	2.4	1.8
R4	1.8	2.1	1.9
R5	2.0	2.2	2.1

After the impact on sandy slopes and the occurrence of moisture anomalies, the sand begins to dry out in contact with atmospheric air, and changes in its physical-mechanical properties are observed. Half an hour after impact, the surface layer moisture drops significantly, in some cases approaching the initial values (R3–R5 series) on average by 0.8%.

## 4. Discussion

### 4.1. Formation and dynamics of moisture anomalies

To establish the correlation between the number of exposure cycles ( $i$ ), initial moisture ( $M_0$ ) and subsequent moisture dynamics ( $M_i$ ), the variation patterns of the moisture anomaly ( $M_a$ ) relative to the number of descents ( $i$ ) visualized in Figure 2 a were calculated. The empirical data obtained allowed to insert a logarithmic model  $0.6\ln(1 + i)$  described by Equation 5 for approximating the detected pattern. Thus, it was demonstrated the possibility of mathematical description of the moisture characteristics evolution of the research object as a function of the intensity of external impact.

The physical meaning of the increment with respect to the number of descents can be explained by the moisture-saturating capacity in relation to the initial moisture for each subsequent descent in the series. As the sand is disturbed, the moisture profile should be aligned with the lower layer of sand that is more moisture-rich.

The empirical values of the moisture anomalies recorded in a sequential sample of measurements show a statistically significant correlation with the number of consecutive descents along the slope, notwithstanding the existence of a substantial amount of statistical emissions (see Figure 2a). The proposed curve clearly demonstrates the non-linear nature of moisture increment under increasing impact. The mixing of sand is noticeable at the first descents, after which there is a significant slowdown in the growth of the moisture anomaly. However, the increase of the moisture anomaly continues to be observed until the maximum number of descents (42 descents in the series). During a series of descents, the lowest layer of sand is successively eroded, which contributes to the addition of moisture to the mixed mass. The low rate of moisture addition due to the greater erosion resistance of the wet compacted naturally formed sands slows down the increase in moisture, which

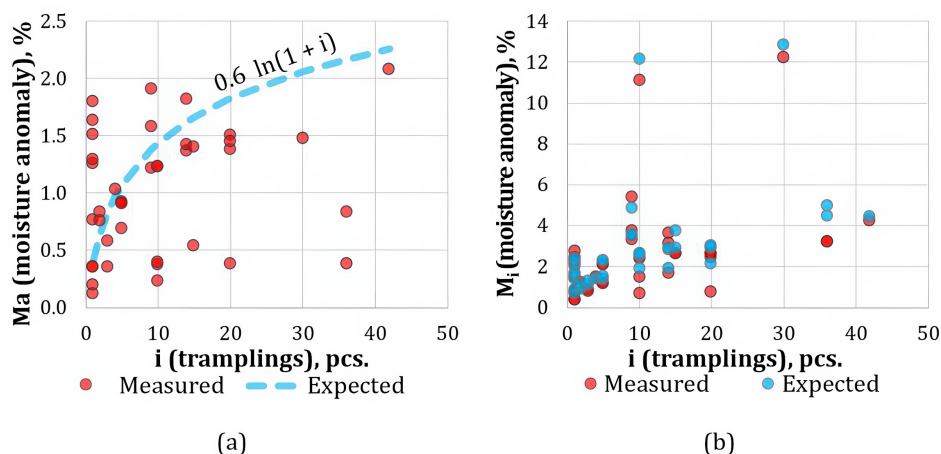


**Figure 2.** Dynamics of measured and expected values according to the model of sand moisture in series of descents. A – moisture anomalies, B – moisture changes in the series of descents.

is reflected in the logarithmic form of the general trend. The sand moisture after  $i$  descents is characterized by Equation 5, which clearly recover the measured values behaviour (see Figure 2b).

$$M_i = M_0 + 0.6 \ln(1 + i), \quad (5)$$

where  $M_i$  is the moisture after  $i$  descents, %;  $M_0$  is the moisture of the surface layer, %;  $i$  is the number of descents, pcs.

#### 4.2. Sand slope dynamics and relief geometric transformation

Human trampling on a sandy slope causes the redeposition of the local volume of sand. In this case, there is an interaction of two processes – a stamp-like squeezing out volume of sand when stepping foot and then its redistribution down the slope (sliding) (Figure 3).

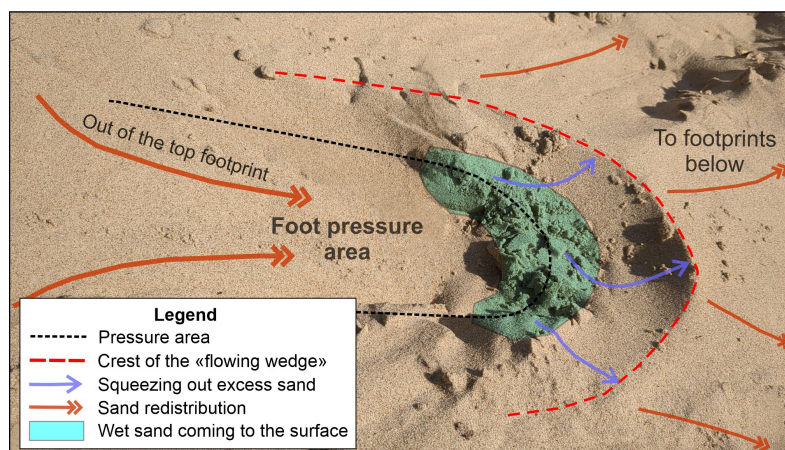


**Figure 3.** Mechanism of sand redistribution when human trampling.

Squeezing the volume of sand by the foot as a stamp forms the effect of “flowing wedge”, in which the limiting channel is formed by chains of tension in the sand mass. Although the flux of sand flows in all directions from the foot, the largest volume is displaced in the direction of slope. This shifting process is localized and ensured by the redistribution of pressure, depending on the moisture and lithological properties of the naturally formed sands, since the self-organized correlated flux is most typical for dry sand. This is most noticeable in the along-slope redistribution of sand from a wave-like ridge of “flowing wedge”, formed by the driest layer (see Figure 3), while moist sand is characterized by spreading.



Thus, the amount of sand moved depends on a combination of factors: the amount of impact (number of descents)  $i$  (Figure 4), slope angle, moisture and lithological properties of the sand, each of which plays its role in the stability of the sandy slope. The combination of these factors' influences on the relief geometric transformation vector  $Q(\text{m}^3/\text{m}) = q/c$  (geometric transformation vector  $q(\text{m}^3/\text{c})$ , brought to a discretization value of 0.05 m), caused by the amount of applied impact  $i$ , can be described by Equation 6:

$$Q(i, M_0, \alpha, D_{50}) = 0.036 \ln(1 + i) + 0.062 M_0 + 0.042 \alpha + 1.045 D_{50}, \quad (6)$$

where  $i$  is the number of descents in a series, pcs;  $\alpha$  is the angle of the sandy slope, degrees;  $M_0$  is the initial moisture of the surface layer, % mass moisture content;  $D_{50}$  is the median diameter, mm.

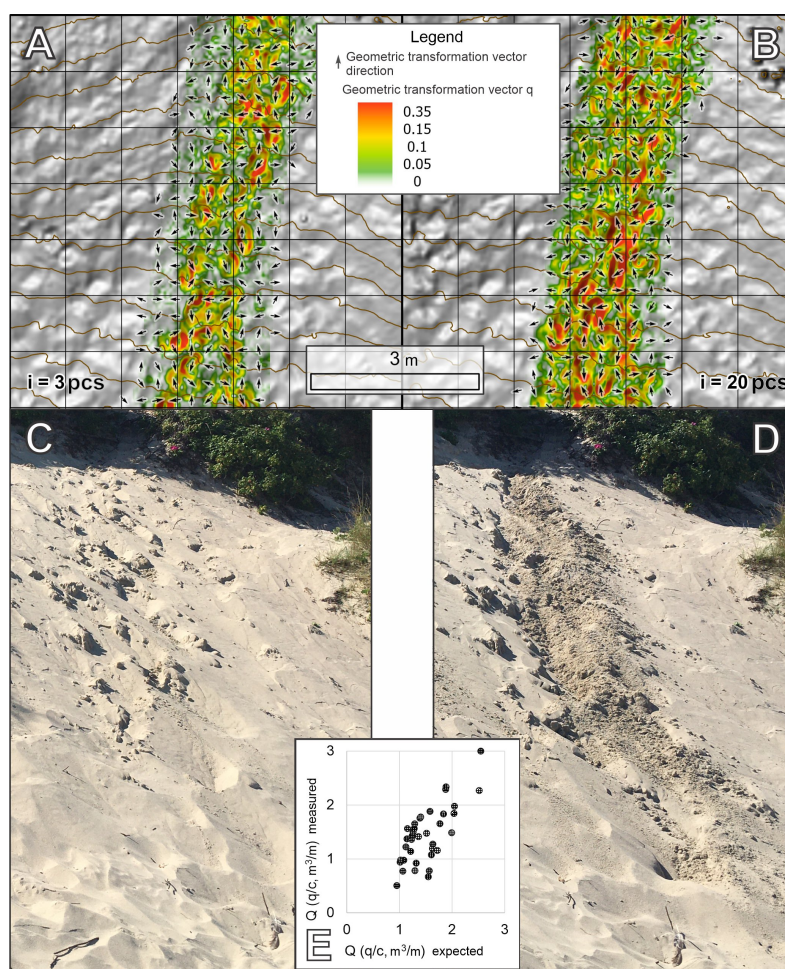


**Figure 4.** Relief geometric transformation vector  $q(\text{m}^3/\text{c}, c = 0.05 \text{ m})$  along the slope with different number of descents and corresponding photo. A and C – geometric transformation vector after  $i = 3$  descents, B and D – geometric transformation vector after  $i = 20$  descents, E – the graph of the measured and expected geometric transformation vector according to Equation 6.

The amount of sand moved when a human descends a sandy slope depends on several factors:

1. Slope angle: the steeper the slope, the more likely the sand will begin to move, the volume redistribution will be more intense and for a longer distance.
2. Sand type: different types of sand have different density and adhesion between particles, for example, the predominance of fine fraction can both lead to the formation of steeper slopes, and increase the sorption capacity of the sand. Wet sand is more resistant than dry, as water increases the bond between grains of sand.

#### 4.3. Role of natural sand drying and formation of erosion instability

With the mechanical anthropogenic impact on sandy slopes application of force occurs impulsively, as in many other exogenous processes. During such impulsive energy inputs, rapid morphological adaptation of the microrelief to new conditions occurs. Due to the cohesion of wet sands, the new topography remains in a reflective state. In morphological dynamics, the relaxation process plays a crucial role as potential energy is redistributed. [Figure 5](#) shows the mechanism of microrelief relaxation after trampling by drying the sand out and crumbling it to the angle of the natural slope.

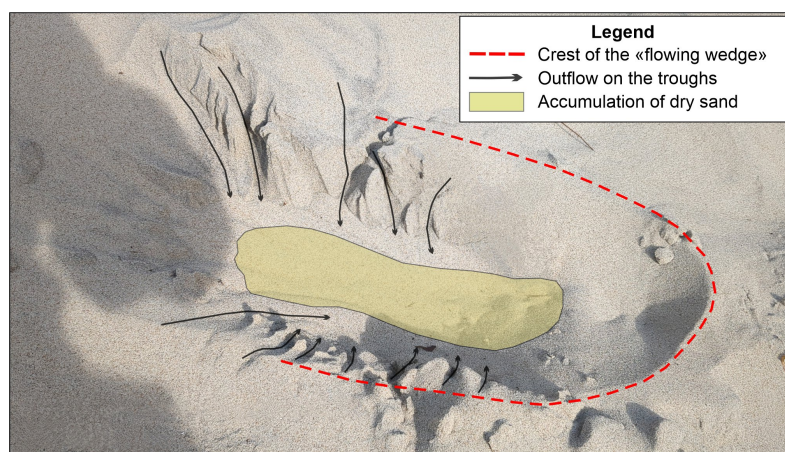


**Figure 5.** Microrelief relaxation in the human footprint on a sandy slope.

The exposed wet sands in [Figure 5](#) are the walls of a wedge-shaped channel formed during the sliding movement of the feet. After the sand is exposed in suitable weather conditions, moisture loss due to evaporation begins. As critical moisture is reached, the process of gradual crumbling begins with the formation of small fluxes in areas of microerosional instabilities, which can appear at this scale conditionally chaotic [Chu *et al.*, 2003]. Eventually, the depth in the wetted sand formed as a result of the foot step is filled with dry sand flowing from the dried areas. Multiple transitions from the reflexive state to the relaxation state within the descent track forms a local moisture anomaly. It can be represented as a depression in the dense moist surface of sand on naturally formed slopes, above which is a layer of dry sand of various thicknesses. For some time, limited by a certain amount of rainfall, the perturbed layer will have a high deflationary potential [Delgado-Fernandez and Davidson-Arnott, 2011; Husemann *et al.*, 2024], which will contribute to the formation of blowouts. Such sand perturbations negatively affect the viability of psammophytes, as their ecological capacity to adapt to similar phenomena is exceeded [Durán and Moore, 2013].

In the long term, due to changes in the physical properties of deeper layers of sand and their multiple local alignment and displacement, the slope is gradually redirected towards new angles and a new “dynamic equilibrium profile” is formed. Such restructuring will be directed only towards reducing the slope, and any opposite changes will occur only at the expense of external processes (aeolian or landslide processes, with elevating and neighboring sections).

#### 5. Conclusion

Based on experimental data from 42 series of controlled descents on natural sandy slopes of coastal dunes 7 m to 10 m in height, it has been established that human trampling cause significant morphodynamic changes. Moisture anomalies in the surface layer reach up to 2.08% (with 42 descents), with the greatest changes after the first 10 impacts. The median diameter of the sand ( $D_{50}$ ) increased by an average of 10  $\mu\text{m}$  to 30  $\mu\text{m}$ , indicating a redistribution of particles and degradation of layers. The maximum recorded relief geometric transformation vector of sand was 3.5  $\text{m}^3/\text{m}$  with 9 descents on slope with an

angle of 46.4°, while on gentle slopes (7.8°) this figure did not exceed 0.5 m<sup>3</sup>/m. These changes form unstable zones with high deflationary activity, especially vulnerable under conditions of climate variability and increasing recreational load. Thus, the results indicate that even moderate recreational use of coastal sandy slopes can provoke processes comparable in scale to natural exogenous forming factors. Recording data on moisture, slope angle and granulometry makes it possible to predict potential erosion zones and make recommendations for the sustainable management of coastal areas.

**Acknowledgments:** The study was funded by a grant from the Russian Scientific Foundation no. 23-77-01039.

## References

- Acosta A. T. R., Jucker T., Prisco I., et al. Passive Recovery of Mediterranean Coastal Dunes Following Limitations to Human Trampling // *Restoration of Coastal Dunes*. — Berlin, Heidelberg : Springer Berlin Heidelberg, 2013. — P. 187–198. — [https://doi.org/10.1007/978-3-642-33445-0\\_12](https://doi.org/10.1007/978-3-642-33445-0_12).
- Bannister A., Raymond S. and Baker R. Surveying. Seventh Edition. — Longman, 1998. — 502 p.
- Belnap J., Phillips S. L., Herrick J. E., et al. Wind erodibility of soils at Fort Irwin, California (Mojave Desert), USA, before and after trampling disturbance: implications for land management // *Earth Surface Processes and Landforms*. — 2007. — Vol. 32, no. 1. — P. 75–84. — <https://doi.org/10.1002/esp.1372>.
- Blott S. J. and Pye K. GRADISTAT: a grain size distribution and statistics package for the analysis of unconsolidated sediments // *Earth Surface Processes and Landforms*. — 2001. — Vol. 26, no. 11. — P. 1237–1248. — <https://doi.org/10.1002/esp.261>.
- Burvingt O. and Castelle B. Storm response and multi-annual recovery of eight coastal dunes spread along the Atlantic coast of Europe // *Geomorphology*. — 2023. — Vol. 435. — P. 108735. — <https://doi.org/10.1016/j.geomorph.2023.108735>.
- Burvingt O., Masselink G. and Russell P. Classification of beach response to extreme storms // *Geomorphology*. — 2017. — Vol. 295. — P. 722–737. — <https://doi.org/10.1016/j.geomorph.2017.07.022>.
- Charbonneau B. R., Duarte A., Swannack T. M., et al. DOONIES: A process-based ecogeomorphological functional community model for coastal dune vegetation and landscape dynamics // *Geomorphology*. — 2022. — Vol. 398. — P. 108037. — <https://doi.org/10.1016/j.geomorph.2021.108037>.
- Chu J., Leroueil S. and Leong W. K. Unstable behaviour of sand and its implication for slope instability // *Canadian Geotechnical Journal*. — 2003. — Vol. 40, no. 5. — P. 873–885. — <https://doi.org/10.1139/t03-039>.
- Cogoni D., Calderisi G., Collu D., et al. Tourist Trampling on a Peripheral Plant Population Restricted to an Urban Natural Area in the Capo Sant’Elia Promontory (Sardinia, W-Mediterranean Basin) // *Plants*. — 2024. — Vol. 13, no. 6. — P. 881. — <https://doi.org/10.3390/plants13060881>.
- Danchenkov A. and Belov N. Comparative Analysis of the Unmanned Aerial Vehicles and Terrestrial Laser Scanning Application for Coastal Zone Monitoring // *Russian Journal of Earth Sciences*. — 2023. — Vol. 23. — ES4008. — <https://doi.org/10.2205/2023es000854>.
- Danchenkov A., Belov N., Bubnova E., et al. Foredune defending role: Vulnerability and potential risk through combined satellite and hydrodynamics approach // *Remote Sensing Applications: Society and Environment*. — 2023. — Vol. 30. — P. 100934. — <https://doi.org/10.1016/j.rsase.2023.100934>.
- Danchenkov A., Belov N. and Stont Z. Using the terrestrial laser scanning technique for aeolian sediment transport assessment in the coastal zone in seasonal scale // *Estuarine, Coastal and Shelf Science*. — 2019. — Vol. 223. — P. 105–114. — <https://doi.org/10.1016/j.ecss.2019.04.044>.
- Danchenkov A. R. and Belov N. S. Morphological changes in the beach-foredune system caused by a series of storms. Terrestrial laser scanning evaluation // *Russian Journal of Earth Sciences*. — 2019. — Vol. 19, no. 4. — ES4003. — <https://doi.org/10.2205/2019ES000665>.
- Defeo O., McLachlan A., Schoeman D. S., et al. Threats to sandy beach ecosystems: A review // *Estuarine, Coastal and Shelf Science*. — 2009. — Vol. 81, no. 1. — P. 1–12. — <https://doi.org/10.1016/j.ecss.2008.09.022>.
- Delgado-Fernandez I. and Davidson-Arnott R. Meso-scale aeolian sediment input to coastal dunes: The nature of aeolian transport events // *Geomorphology*. — 2011. — Vol. 126, no. 1/2. — P. 217–232. — <https://doi.org/10.1016/j.geomorph.2010.11.005>.
- Durán O. and Moore L. J. Vegetation controls on the maximum size of coastal dunes // *Proceedings of the National Academy of Sciences*. — 2013. — Vol. 110, no. 43. — P. 17217–17222. — <https://doi.org/10.1073/pnas.1307580110>.



- Eelsalu M., Parnell K. E. and Soomere T. Sandy beach evolution in the low-energy microtidal Baltic Sea: Attribution of changes to hydrometeorological forcing // *Geomorphology*. — 2022. — Vol. 414. — P. 108383. — <https://doi.org/10.1016/j.geomorph.2022.108383>.
- Fenu G., Cogoni D., Ulian T., et al. The impact of human trampling on a threatened coastal Mediterranean plant: The case of *Anchusa littorea* Moris (Boraginaceae) // *Flora - Morphology, Distribution, Functional Ecology of Plants*. — 2013. — Vol. 208, no. 2. — P. 104–110. — <https://doi.org/10.1016/j.flora.2013.02.003>.
- Folk R. L. and Ward W. C. Brazos River bar [Texas]; a study in the significance of grain size parameters // *Journal of Sedimentary Research*. — 1957. — Vol. 27, no. 1. — P. 3–26. — <https://doi.org/10.1306/74D70646-2B21-11D7-8648000102C1865D>.
- Hesp P., Schmutz P., Martinez M. M., et al. The effect on coastal vegetation of trampling on a parabolic dune // *Aeolian Research*. — 2010. — Vol. 2, no. 2/3. — P. 105–111. — <https://doi.org/10.1016/j.aeolia.2010.03.001>.
- Hesp P. A. The Formation of Deflation Ridges // *Marine Geology*. — 2024. — Vol. 475. — P. 107367. — <https://doi.org/10.1016/j.margeo.2024.107367>.
- Husemann P., Romão F., Lima M., et al. Review of the Quantification of Aeolian Sediment Transport in Coastal Areas // *Journal of Marine Science and Engineering*. — 2024. — Vol. 12, no. 5. — P. 755. — <https://doi.org/10.3390/jmse12050755>.
- Liddle M. J. and Greig-Smith P. A Survey of Tracks and Paths in a Sand Dune Ecosystem I. Soils // *The Journal of Applied Ecology*. — 1975. — Vol. 12, no. 3. — P. 893–908. — <https://doi.org/10.2307/2402097>.
- Mather A. S. and Ritchie W. The beaches of the Highlands and Islands of Scotland. — Countryside Commission for Scotland, 1977.
- Moskalewicz D., Bahr F., Janowski L., et al. Morphology and internal structure of small-scale washovers formed in the coastal zone of the semi-enclosed tideless basin, Gulf of Gdańsk, Baltic Sea // *Geomorphology*. — 2024. — Vol. 463. — P. 109368. — <https://doi.org/10.1016/j.geomorph.2024.109368>.
- Nordstrom K. F. Beaches and Dunes of Developed Coasts. — Cambridge University Press, 2000. — <https://doi.org/10.1017/CBO9780511549519>.
- Pessoa M. F. and Lidon F. C. Impact of human activities on coastal vegetation ? A review // *Emirates Journal of Food and Agriculture*. — 2013. — Vol. 25, no. 12. — <https://doi.org/10.9755/ejfa.v25i12.16730>.
- Pinna M. S., Bacchetta G., Cogoni D., et al. Is vegetation an indicator for evaluating the impact of tourism on the conservation status of Mediterranean coastal dunes? // *Science of The Total Environment*. — 2019. — Vol. 674. — P. 255–263. — <https://doi.org/10.1016/j.scitotenv.2019.04.120>.
- Ravichandran K. and Rashid R. A. A review of recreational trampling impact on nature trail // *Universiti Putra Malaysia*. — 2017. — Vol. 10, no. 2. — P. 2–7.
- Sibson R. A brief description of natural neighbour interpolation // *Interpreting multivariate data*. — John Wiley & Sons, 1981. — P. 21–36.
- Stont Z. I., Bobykina V. P. and Ulyanova M. O. "Diving" cyclones and consequences of their impact on the coasts of the South-Eastern Baltic Sea // *Russian Journal of Earth Sciences*. — 2023a. — Vol. 23, no. 2. — ES2001. — <https://doi.org/10.2205/2023ES000827>.
- Stont Z. I., Esiukova E. E. and Ulyanova M. O. Clusters of Cyclones and Their Effect on Coast Abrasion in Kaliningrad Region // *Russian Journal of Earth Sciences*. — 2023b. — Vol. 23, no. 3. — ES3008. — <https://doi.org/10.2205/2023es000826>.
- Williams R. DEMs of difference // *Geomorphological techniques*. — 2012. — Vol. 2, no. 3.2.